

Detection and Digital Modeling of Subsurface Pipe Structures from Ground Penetration Radargrams

Ralf Becker¹, Simon Dörr¹, Yannick Fahlenbock², Luisa Kahlert², Hristo Vassilev¹, Jörg Blankenbach¹

¹Geodetic Institute and Chair for Computing in Civil Engineering & GIS, RWTH Aachen University, Germany

²GeoRADAR NRW GmbH & Co. KG., Germany
ralf.becker@gia.rwth-aachen.de

Abstract. The introduction of Building Information Modelling (BIM) has allowed practitioners in the construction industry to efficiently exchange information between different disciplines. Nevertheless, planning still relies on incomplete as-is information about subsurface objects, which is especially problematic in conversion areas. Therefore, to facilitate the digital planning process we present a workflow, which processes and interprets radargrams, produced with ground-penetrating radar (GPR) data into standardized formats such as CityGML Utility Network ADE and Industry Foundation Classes (IFC) by creating modelling tools aimed towards the generation of subsurface pipeline information models.

1. Introduction

The detailed knowledge of the objects found in the soil (e.g., pipelines for supply and disposal, remaining cellars, shafts or explosive ordnance from the last world war) is essential for the (residential) redevelopment of e.g., previously industrially used areas (conversion areas) or also the subsequent densification of residential development. This is especially true if they are not to be disposed of as in contaminated sites, but rather must be preserved or connected to in the course of a redesign. For efficient and seamless digital planning, these objects should already be included in an early as-is model. However, as-is plans of e.g., pipe networks, remaining basements or shafts are often inaccurate, only available in analog form or missing completely. Furthermore, screening the subsurface for such objects is currently only possible with extremely time-consuming and costly (manual) efforts (e.g., by excavation).

The research project “GPR2BIM” aims to enable the non-destructive and non-contact detection and capture of objects present in the ground. Using pipelines as an example and by linking the technology of Ground-penetrating Radar (GPR), Geographic Information Systems (GIS) and the method of Building Information Modeling (BIM) the goal is to create a workflow that is as automated as possible (Figure 1).

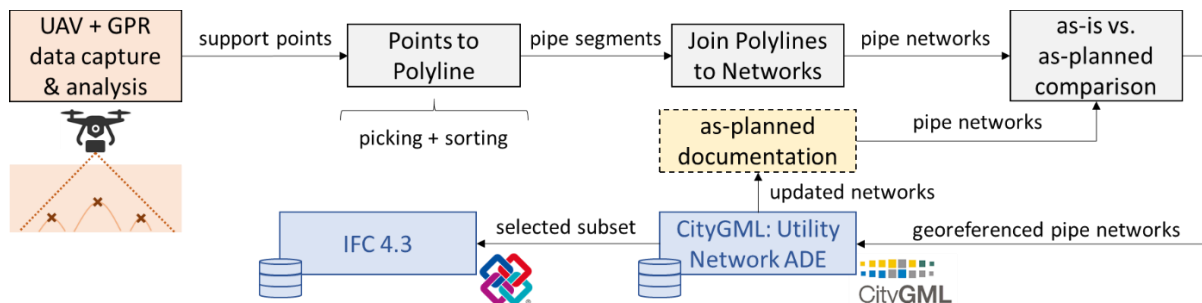


Figure 1: Capturing, modelling and analysis of pipe systems in GPR2BIM

2. State of the Art

2.1 GPR data capture

The geophysical method GPR is an impulse reflection technique (Daniels, 2005) and is a tool for subsurface imaging since several decades. It has developed into an aide in civil engineering by trying to avoid the damage of various subsurface structures like archaeological sites or conduits. Surveys are usually performed with the transmitting and receiving antennas arranged with a fixed offset dragged close to the surface (Annan, 2009). Since diffractions of an object smaller than the wavelength of the pulse produce characteristic hyperbolas (Linford, 2006), the crossing of most pipes and lines is easily identified in radargrams.

Still being subject to restriction, the use of Unmanned Aerial Vehicles (UAV) mounted GPR antennas has reached the commercial field (Francke and Dobrovolskiy, 2021). While the approach of individual designs (like Vivaldi antennas) is used for applications like landmine and IED detection (Fernández et al., 2021) commercial manufacturers offer antennas that can be used in ground-coupled as well as in drone-mounted mode (Noviello et al., 2022). Advantages of autonomous flights are the possibility to predefine reproducible routes and produce evenly spaced parallel profiles. In situations that are potentially dangerous for an operator UAVs can lower the risks of injuries (Chandra and Tanzi, 2018).

The use of autonomous UAV in geophysical applications is limited by different factors. First, there are legal restrictions concerning both the UAV itself and the GPR antenna (Francke and Dobrovolskiy, 2021). Then, there are technical limitations of the different parts of the unmanned aircraft vehicle e.g., maximum take-off mass, precision of positioning, reduced air time due to payload weight. Lastly, by using GPR antennas in an air-launched configuration the data presents differently than in conventional, ground-coupled settings. For instance, the lateral resolution is reduced and the amplitude of the target reflection is decreased (Diamanti and Annan, 2017).

2.2 GPR data analysis

In order to improve the visibility of reflections and depict every feature at the most precise location, the raw data can be processed. Typical steps are gains to counteract the attenuation of the electromagnetic wave (Cassidy and Jol, 2009), and frequency filters and spatial filters to eliminate electromagnetic signals from other sources and horizontal striping, respectively (Sandmeier, 2014). By deconvolving the source wavelet from the scan, it is tried to gain the Earth's impulse response (Kearey et al., 2002). Migration processing is used to move reflectors to their real origin and to contract hyperbolas to a single point (Cassidy and Jol, 2009).

Once the data is processed it can be interpreted. In the case of pipes and lines this means that local maxima above a certain value are picked. The pick has a travel-time, which can be converted to depth with the knowledge of the wave velocity (Linford, 2006), and a scan number, which can be converted to horizontal positioning. The previous approach is to assign picks to certain pipes as well as possible and to assume straight courses between the given points. Distances between points depend on real life circumstances and can be between centimetres and up to tens of meters (e.g. pipelines).

2.3 Pipeline network generation and CityGML

CityGML¹ is an open data model and XML-based format for the representation and exchange of 3D city models. It is an international standard developed by the Open Geospatial Consortium (OGC) and provides a common language for the exchange of 3D urban information. The CityGML schema defines a set of classes and attributes that can be used to represent the different aspects of a city, including buildings, streets, public spaces, and infrastructure. A key feature of CityGML are Application Domain Extensions (ADEs), which extend the model with additional classes and attributes, which are then specific to their application domain.

The ADE used in this work – Utility Network ADE (Becker et al., 2011) – was mainly developed to investigate failure-related cascade effects of interconnected supply networks (SIMKAS 3D, 2013). The main concept of the format is the modelling approach of dual representation. The approach is described as the possibility that a network feature can be described both, by its 3D topography and by means of a complementary graph structure called `FeatureGraph`. This means that a logical representation of the real world is used in addition to the spatial representation. The logical integration of an object into its environment can also take place when modelling in space would not be possible due to missing positional data, or where it is not necessary. For example, the functionality of a (water-) pump can be linked to the functionality of a power point without having to model the physical cable connecting the two objects. With the given possibilities of the ADE, objects can be combined into different supply networks (the term refers in this context to a homogeneous medium in each case) and their interdependencies can be represented.

If the geospatial data of a utility network is already available, it is possible to create a Utility Network ADE compliant data by file conversion. (Boates et al. 2017) and (Den Duijn et al. 2018) created models of utility networks provided by local authorities as geodata using the conversion tool Feature Manipulation Engine (FME) by Safe Software Inc. In such a transformation, special attention must be paid to the correct generation of logical connections during the semi-automated transformation.

2.4 Integration of the data and results into a digital 3D BIM model

Incorporating GIS data from a format such as CityGML into standardized data models from the AECO domain like IFC has challenges on a georeferencing, semantical and geometric level: firstly, in CityGML all coordinates belong to a geodetic or spatial reference system (SRS) and local transformations are not permitted (Herle et al., 2020). IFC has a different scope and a different scale, mainly focusing on single sites with each object within them defined in a local Cartesian coordinate system relative to a superordinate spatial structure in which they are placed (Borrmann et al., 2018). Therefore, (Salheb et al., 2020) propose an approach to transition from geodetic (here the Universal Transverse Mercator (UTM) coordinates of a CityGML file by finding the smallest coordinates in the scene and using that point as the origin of a local project coordinate system (PCS) of the IFC construction site object (`IfcSite`). This is the simplest way to georeference IFC models, but is sufficient for embedding the data in GIS in first step (Clemen et al., 2022). For large-scale models IFC 4.0 (or higher) includes furthermore the possibility for the definition of a 2D-Helmert transformation, the parameters of which can be encapsulated in a `IfcMapConversion` object (Clemen et al., 2022)

When it comes to semantics and geometric representations the two standards (IFC and CityGML) differ significantly in their definitions. For example, geometries are represented in CityGML by using boundary representations (B-Rep), while IFC mostly relies on constructive

¹ <https://www.ogc.org/standard/citygml/>

solid geometry (CSG). This is usually solved through either linking or transforming. The linking approach for semantic interoperability consists of first translating both file formats into a Resource Description Framework (RDF) graph and subsequently integrating those using semantic web technologies (Hor et al., 2016). This does not change the file structure but introduces additional need for maintenance of the linked model. Alternatively using a set of rules, the data can be transformed from CityGML to IFC and vice versa. However, this should be done with caution and on a case by case basis, since due to the different paradigms, the transformation leads to a loss of detail and information (Herle et al., 2020). Specifically in the domain of underground pipe infrastructure, (Hijazi et al., 2011) show promising results about the integration of the previously mentioned Utility Network ADE extension for CityGML into IFC for the purpose of extending the state documentation of public utilities and pipelines with as-planned indoor information from BIM models of individual buildings.

3. Methodology

3.1 GPR data capture

In order to test the response of different pipes and objects, a test site was built containing structures with varying materials and depths (below surface). The pipes were laid at three different depth levels: 50 cm, 1 m and 1.5 m. With three objects placed on the uppermost layer, four on the medium level and eight in the deepest part of the pit. While the hole was still open, both a georeferenced orthophoto and laser scan point cloud were created. Digital models of the pipes were derived from the latter (Figure 2). Most objects (Table 1) are air-filled plastic pipes with diameters between 5 cm and 30 cm. The exceptions are number 4, which is a solid metal rod, and number 15, which are three touching parallel pipes. The row of paving stones that can be seen next to number 16 did not qualify for comparison in the laser scan measurement.



Figure 2: Orthophoto of the test site with numbered objects.

Table 1: Characterization of the different objects.

Number	Material	Diameter	Depth layer
1	Polyethylen	30 cm	150 cm
2	Polyethylene	30 cm	150 cm
3	Polyvinyl chloride	16 cm	150 cm
4	Metal	5 cm	150 cm
5	Polyvinyl chloride	11 cm	150 cm
6	Polyethylene	7 cm	150 cm
7	Polyethylene	12 cm	150 cm
8	Polyethylene	16 cm	150 cm
9	Polyethylene	12 cm	100 cm
10	Polyethylene	12 cm	100 cm
11	Polyethylene	12 cm	100 cm
12	Polyvinyl chloride	12 cm	100 cm
15	Polyethylene	3x5 cm	50 cm
16	Polyethylene	5 cm	50 cm

In order to compare the UAV data in different flight heights with a reference later on, we first gathered a data set in a ground-coupled survey only days after the installation of the test site. The employed array system consists of 18 channels (impulseRadar raptor) with a centre frequency of 450 MHz. Although the spacing of 8.3 cm between the channels usually constitutes a feasible in-line sample spacing, the test site was passed lengthwise and crosswise. This way for every object there will be enough perpendicular radargrams in order to obtain a sufficient number of picks for each structure. Here the GPR antennas are placed as close to the surface as possible. The positioning is ensured with one Real-time kinematic Global Navigation Satellite System (RTK GNSS) receiver. The paths of all 18 channels are calculated with fixed distances from this center position.

The UAV setup is shown in Figure 3. The Ground Control software (UgcS²) is used to plan the flight route which is then downloaded by the remote control and uploaded to the drone. The remote control is also necessary to intervene in hazardous situations. When triggered, the UAV can fly the complete course autonomously. For a precise positioning the GNSS receiver of the vehicle is connected to a GNSS base station enabling RTK corrected location data. This data is transferred to the GPR data logger, which in turn collects and stores the GPR scans with the associated positioning. Since a constant distance to the surface is important the system is equipped with an altimeter. First survey tests are done, but have to be improved with further surveying campaigns.

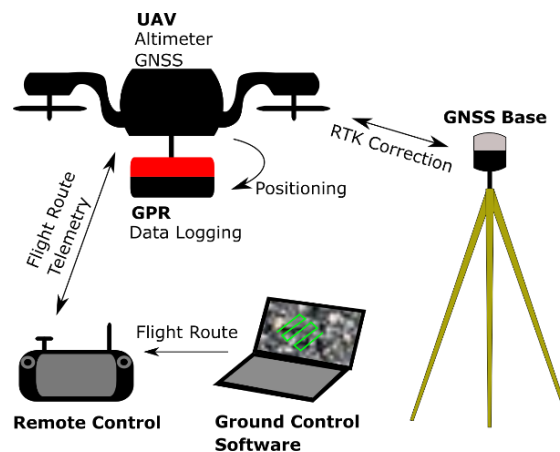


Figure 3: UAV setup.

3.2 GPR data analysis

During the first ground-coupled reference survey at the test site 12 objects were successfully detected. The pipes and objects can already be identified in amplified raw data. However, a standard processing procedure was applied to the data to improve the picking precision.

After a gain and a time-zero correction was applied, the data was filtered with a bandpass filter and a spatial filter (background removal) to remove very high and very low frequency noise as well as horizontal striping. After deconvolution the signal appeared to be sharper and after migrating and a Hilbert transform the reflection hyperbolas of the objects were contracted to local maxima in the radargrams, which further facilitates the picking process (Figure 4). All radargrams were examined both after the last processing step and after the deconvolution, which helps to inspect the shape of the hyperbola, which is characteristic for profiles crossing a pipe. All visible reflections were picked and stored as points with their three-dimensional position.

² <https://www.ugcs.com/>

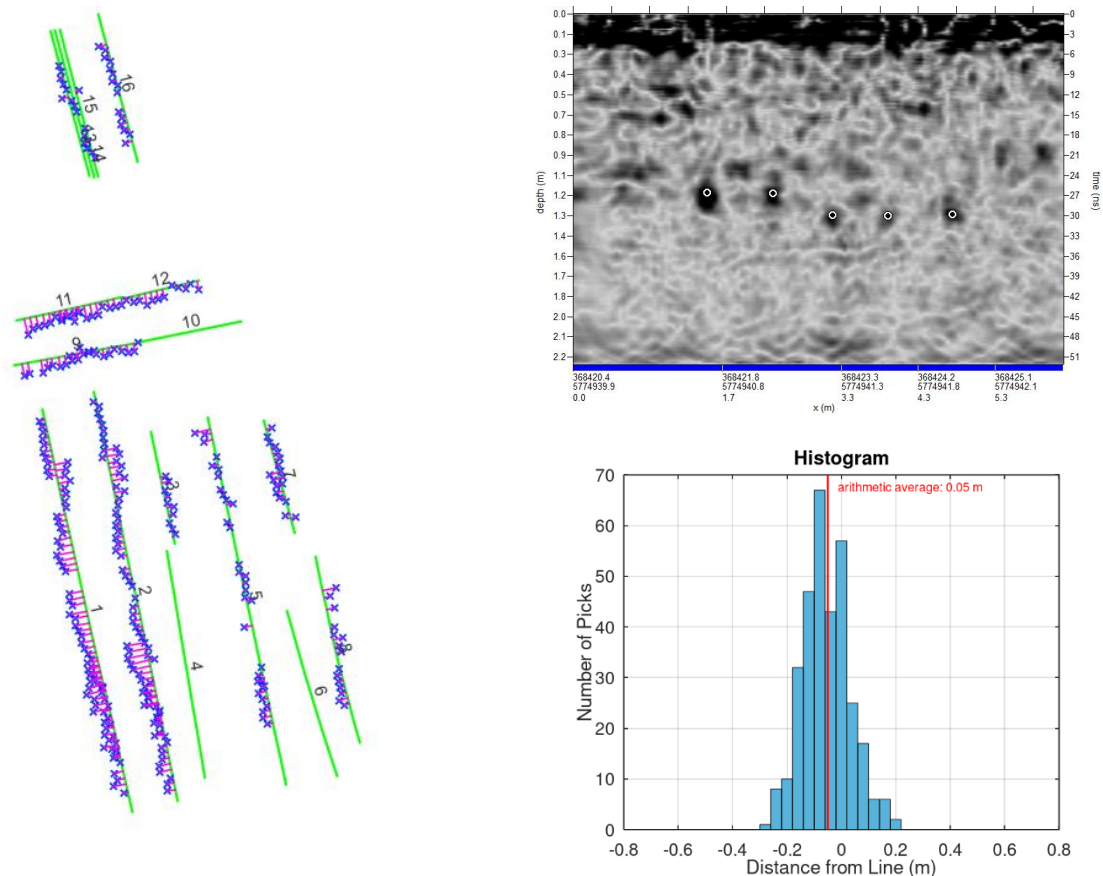


Figure 4: left - true location of the pipes and objects (green) with picks (blue) and in-line distance (magenta); upper right - radargram with picks; lower right - histogram of in-line distances of all pipes

Of the 14 pipes and objects, only two could not be identified in the GPR data. Pipe 10 was detected, but since one end of it was moved during the filling of the hole, it is not usable for the comparison. The metal rod 4 and pipe 6 were not visible on the radargrams because of their depth/diameter ratio.

We determined the horizontal distance of each pick to the laser scan derived line. That means the in-line distance of the intersection of the profile was subtracted from the in-line distance of the pick. The resulting average differences are negative for all objects and the arithmetic mean of all distances is -18 cm. This value did not correspond to the usual deviation and led to a review of the radar data positioning. It was found that the allocation of the individual samples was incorrect and that the allocation could be improved by using different settings in the third-party software. After this, with an average of -5 cm the difference (Figure 4 lower right) is in the range of typical GPR measurements and can serve as an example for fitting.

3.3 Automatized pipeline network generation

In order to open up the possibility of automated collection and processing of the georadar data, a plug-in for the open GIS software QGIS³ was created within the context of this project, with which objects with assigned properties in the sense of the CityGML Utility Network ADE can be created from the extracted coordinates. During the development we concentrated on the implementation of the object classes for utility lines. The utility lines can be provided with all available attributes and can be combined to form networks. In addition to the topographical

³ <https://www.qgis.org/de/site/>

representation, this also preserves the logical representation. The result of processing the georadar data with the developed plugin is an exportable file in Geography Markup Language (GML) format that is valid in the sense of the Utility Network ADE (0.9.3). The created networks can be extended in future sessions, loaded for viewing in other software or used for graph-theoretical network analysis. Coordinate sets stored in CSV format, containing preselected points, serve as the starting point for processing with the developed plugin. They are currently extracted from radargrams in a preceding, manual work step; a radargram corresponds to the visualization of the data of a measurement of an antenna on the radar setup. Conspicuous reflection shapes are identified and their coordinates are exported. The user also has the option of adding a comment (tag) in which the most probable cause of the reflection (utility lines, foundations, boulders, etc.) can be encoded.

With this type of presorting, the difficulty arises that only two-dimensional sections of the overall three-dimensional image can be viewed at a time. This can limit the understanding of how the selected positions are related to each other. As soon as the coordinate collections are imported into QGIS, the typical GIS top view results in an overview that contains data from the entire survey area. Using the various filtering methods, it is now possible to sort by for example special tags, signal intensities or altitudes. Together with the use of map material (e.g. visualizations of the interpolated radar measurements) of the survey site, educated guesses can be made about the exact location of the supply lines to be located.

In a first step, individual line sections are identified and combined into objects (`featureGraph`). For this purpose, an individual subset of points is selected and automatically sorted. The sorting is done by a specially developed algorithm and is effective for all line-like objects. Finally, the set of all objects created corresponds to the network to be created. Behind the user interface, the “pandas”⁴ library is used for this purpose. Data frames are created, each of which contains the data of a utility line section. In addition to the coordinates and unique names, these data frames also contain columns for all attribute values that can be added in the further course of editing, which the Network Utility Picker ADE provides for objects of the utility line type.

The described way of creating utility line objects uses the point coordinates initially loaded as supporting points of the entities to be created. It happens that the survey in the field cannot be carried out with sufficient accuracy to capture objects hidden underground in their entirety. In this case, not enough points are generated to virtually describe the objects with sufficient accuracy. If, however, their positions can be estimated in post-processing on the basis of further indications, support points can be added manually. Data sets that are changed manually will be marked accordingly. Once all the desired line objects have been created, connections (`interFeatureLink`) can then be created between the objects. In the process, the end of a line object can always be linked to any support point or a coordinate created by interpolation between two support points of another line object. A line object never extends beyond a connection point, but is divided accordingly.

Finally, attribute values for the properties provided in the Utility Network ADE can be assigned to the line objects. Once all objects have been created, linked and provided with the necessary properties, the current project can be temporarily saved in a CSV file, which can be imported by a corresponding function of the plug-in, or a valid GML file can be exported.

3.4 As-is versus as-planned comparison

As discussed, a common problem for as-is documentation is that it’s often incomplete or inaccurate. In order to facilitate the merging process of an as-is model done through a GPR

⁴ <https://pandas.pydata.org/>

survey with an existing documentation a procedure was developed to detect spatial matches between two sets of 3D polyline or spline objects. The algorithm considers pairs of curves from each set, subdivides the curve from the first set at regular intervals and projects the subdivisions on the pair from the opposite set. A discrepancy score is calculated based on the root mean square of the distances to the projections. Based on this score a threshold can be used to mark polylines that do not match and would need to be handled manually by the user.

3.5 Integration of the data and results into a digital 3D BIM model

Translating CityGML to IFC

After the survey data have been collected, analysed and stored in a CityGML Utility Network ADE database the next step considers the scenario in which a limited subset shall be extracted and converted to the IFC format, utilizing the open-source library “ifcopenshell”⁵, for the purpose of serving as a reference for the planning of construction or retrofitting works. As previously discussed the UTM coordinates of CityGML need to be transformed into a local PCS. As mentioned in section 2.4 we implement a common approach of iterating through all points to find the minimum UTM coordinates and setting this as the origin of the PCS. Using the EPSG code defined in the CityGML model, we transform the UTM coordinates of the PCS origin to geographic coordinates of WGS84 (longitude, latitude) and provide this information to the `IfcSite` object. The UTM coordinates of each individual feature in the CityGML data is then reduced translationally using the UTM coordinates of the PCS origin. The result of these steps is validated in a CityGML enabled BIM viewer software (FZK Viewer⁶), showing that both models perfectly overlap each other.

With the origin and the PCS defined, we then iterate through the previously described hierarchical structure of the Utility Network ADE with the goal of transforming it into IFC with the least possible loss of semantic and geometric information. Instead of linked nodes piping and utilities in IFC are represented by subclasses of the class `IfcDistributionElement`. Their endpoints are represented by an `IfcDistributionPort`, which can then be connected to the ports of other utilities by the non-physical relationship `IfcRelConnectsPorts`. In order to preserve the grouping hierarchy of Utility Network ADE the `FeatureGraph` and `Network` objects are translated to a nested series of `IfcSystem` objects, which themselves also have input and output ports and can therefore serve an equivalent purpose. In addition, an optional flow direction can be supplied as a property of the distribution ports in IFC. Although the two formats differ in their supported geometry types, in the case of GPR scans this does not pose a serious issue, since the resulting sparse point cloud cannot represent geometric detail. Instead, two viable choices for representing linear objects are available in IFC: `IfcLine` for simply representing the axis of a pipe and `IfcExtrudedAreaSolid` generating an extruded 3D-object in the case of a known profile shape and size.

Line fit quality

An alternative approach to using the GPR-picks directly as nodes of the network, is approximating a line after pre-segmenting the points into linear segments with a single predominant direction. To this end we use a Hough transform for pre-segmentation (Dalitz et al., 2017) followed by least squares for refined fitting (Figure 5). These two steps allow noise and outliers to be filtered out but may lead to loss of information about how good the fit is. Fortunately, IFC provides a predefined property set - `Pset_Uncertainty`, which can be used to

⁵ <https://ifcopenshell.org/>

⁶ <https://www.iai.kit.edu/1648.php>

capture the geometric uncertainty of building parts. We use the standard deviation of the residuals as linear uncertainty. We further split the residuals into horizontal and vertical uncertainty, due to the fact that these are each caused by different mechanisms in the measurement process.

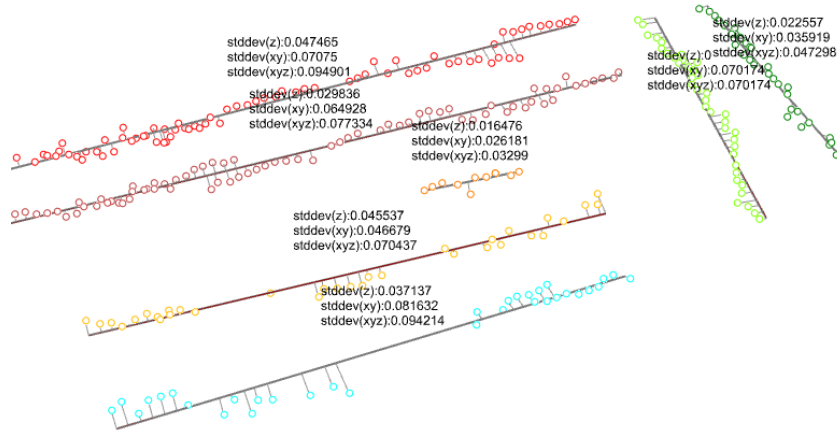


Figure 5: Segmentation and line fitting through the dataset of our test field

4. Conclusion and outlook

With this work we presented a workflow, that aims to investigate the subsurface of conversion areas. We have shown through empirical testing, that the ground-coupled GPR can detect pipe objects made with common materials at different depths. With our UAS setup we have achieved promising early results, which need to be improved upon in further work. We facilitate the interpretation of the radargrams by a processing step, after which the picked points are gathered in a georeferenced point cloud with the detected subsurface objects. In order to distinguish pipe networks, the data is brought into a GIS software, for which we developed a plug-in, that can output pipeline information in the NetworkADE format extension of CityGML. Additionally, our tools can perform a comparison with the existing documentation to show missing or inaccurate objects. For the purpose of integrating the data in as-is models of construction projects we developed a format translation tool, which can output subsets of the CityGML model as IFC. Up to now, basis of our investigations is the ground-coupled GPR, but in the next steps we will expand our examinations to the described UAV GPR approach.

5. Acknowledgements

We acknowledge the funding of the GPR2BIM project by the Federal State of North Rhine-Westphalia within the program (03G0847A).

6. References

- Annan, A., (2009). Electromagnetic principles of groundpenetrating radar. In: *Ground penetrating radar: theory an dapplications*. s.l.:Elsevier.
- Becker, T., Nagel, C., Kolbe, T.H., 2010: SIG 3D Special interest Group 3D - Modeling group - UtilityNetworkADE - Core Model Draft Version 0.1.0

- Boates, I., Aguiaro, G., Nischersu, A. (2018). Network Modelling and Semantic 3D City Models: Testing the Maturity of the utility Network ADE for CityGML with a water network test case. <https://doi.org/10.5194/isprs-annals-IV-4-13-2018>
- Borrmann, A., König, M., Koch, C., & Beetz, J. (2018). Building information modeling: Technology foundations and industry practice. *Building Information Modeling: Technology Foundations and Industry Practice*, 1–584. <https://doi.org/10.1007/978-3-319-92862-3>
- Bosché, F. (2010). Automated recognition of 3D CAD model objects in laser scans and calculation of as-built dimensions for dimensional compliance control in construction. *Advanced Engineering Informatics*, 24(1), 107–118. <https://doi.org/10.1016/j.aei.2009.08.006>
- Cassidy, N. J., & Jol, H. M. (2009). Ground penetrating radar data processing, modelling and analysis. *Ground penetrating radar: theory and applications*, 141–176.
- Clemen, C.; Becker, R.; Kaden, R.; Blankenbach, J. (2022): Georeferenzierung. In: Kaden, R.; Clemen, C.; Seuß, R.; Blankenbach, J.; Becker, R.; Eichhorn, A., Donaubaue, A.; Kolbe, T.H., Gruber, U. (Herausgeber): Leitfaden Geodäsie und BIM, Version 3.1, S. 50-65, 978-3-95786-323-2 (Printversion), DVW Gesellschaft für Geodäsie, Geoinformation und Landmanagement e.V., Runder Tisch GIS e.V. (2022), DVW – Merkblatt 11-2022. <http://www.dvw.de/BIM-Leitfaden.pdf>
- Dalitz, C., Schramke, T., & Jeltsch, M. (2017). Iterative Hough Transform for Line Detection in 3D Point Clouds. *Image Processing On Line*, 7, 184–196. <https://doi.org/10.5201/ipol.2017.208>
- Den Duijn, X., Aguiaro, G., Zlatanova, S. (2018). Modelling below- and above-ground utility network features with the CityGML Utility Network ADE: Experiences from Rotterdam <https://doi.org/10.5194/isprsannals-IV-4-W7-43-2018>
- Diamanti, N., & Annan, A. P. (2017, March). Air-launched and ground-coupled GPR data. In *2017 11th European Conference on Antennas and Propagation (EUCAP)* (pp. 1694-1698). IEEE.
- Francke, J., & Dobrovolskiy, A. (2021, September). Challenges and opportunities with drone-mounted GPR. In *First International Meeting for Applied Geoscience & Energy* (pp. 3043-3047). Society of Exploration Geophysicists.
- Fernández, M. G., Narciandi, G. Á., Arboleya, A., Antuña, C. V., Andrés, F. L. H., & López, Y. Á. (2021). Development of an airborne-based GPR system for landmine and IED detection: Antenna analysis and intercomparison. *IEEE Access*, 9, 127382-127396.
- Herle, S., Becker, R., Wollenberg, R., & Blankenbach, J. (2020). GIM and BIM: How to Obtain Interoperability Between Geospatial and Building Information Modelling? *PFG – Journal of Photogrammetry, Remote Sensing and Geoinformation Science*, 88(1), 33–42. <https://doi.org/10.1007/s41064-020-00090-4>
- Hijazi, I., Ehlers, M., Zlatanova, S., Becker, T., & van Berlo, L. (2011). Initial Investigations for Modeling Interior Utilities Within 3D Geo Context: Transforming IFC-Interior Utility to CityGML/UtilityNetworkADE. In T. H. Kolbe, G. König, & C. Nagel (Hrsg.), *Advances in 3D Geo-Information Sciences* (S. 95–113). Springer Berlin Heidelberg. https://doi.org/10.1007/978-3-642-12670-3_6
- Hor, A.-H., Jadidi, A., & Sohn, G. (2016). BIM-GIS Integrated Geospatial Information Model Using Semantic Web and RDF Graphs. *ISPRS Annals of Photogrammetry, Remote Sensing and Spatial Information Sciences*, III-4, 73–79. <https://doi.org/10.5194/isprsannals-III-4-73-2016>
- Linford, N. (2006). The application of geophysical methods to archaeological prospection. *Reports on progress in physics*, 69(7), 2205.
- Salheb, N., Arroyo Otori, K., & Stoter, J. (2020). Automatic Conversion of CityGML to IFC *The International Archives of the Photogrammetry, Remote Sensing and Spatial Information Sciences*, XLIV-4/W1-2020, 127–134. <https://doi.org/10.5194/isprs-archives-XLIV-4-W1-2020-127-2020>
- Sandmeier, K. (1998). Windows™ 9x/NT/2000/XP/7-program for the processing of seismic, acoustic or electromagnetic reflection, refraction and transmission data.
- SIMKAS 3D (2012): Bundesministerium für Bildung und Forschung - SIMKAS 3D: Simulation von intersektionellen Kaskadeneffekten bei Ausfällen von Versorgungsinfrastrukturen unter Verwendung des virtuellen 3D-Stadtmodells von Berlin